



Published in final edited form as:

J Neurooncol. 2016 January ; 126(2): 317–325. doi:10.1007/s11060-015-1970-3.

Tryptophan PET Predicts Spatial and Temporal Patterns of Post-Treatment Glioblastoma Progression Detected by Contrast-Enhanced MRI

Edit Bosnyák^{1,6}, David O. Kamson^{1,6}, Natasha L. Robinette^{2,7}, Geoffrey R. Barger^{3,7}, Sandeep Mittal^{4,5,7}, and Csaba Juhász^{1,3,6,7}

¹Department of Pediatrics, Wayne State University, Detroit, MI, USA

²Department of Radiology, Wayne State University, Detroit, MI, USA

³Department of Neurology, Wayne State University, Detroit, MI, USA

⁴Department of Neurosurgery, Wayne State University, Detroit, MI, USA

⁵Department of Oncology, Wayne State University, Detroit, MI, USA

⁶PET Center, Children's Hospital of Michigan, Detroit, MI, USA

⁷Karmanos Cancer Institute, Detroit, MI, USA

Abstract

Background—Amino acid PET is increasingly utilized for the detection of recurrent gliomas.

Increased amino acid uptake is often observed outside the contrast-enhancing brain tumor mass. In this study, we evaluated if non-enhancing PET+ regions could predict spatial and temporal patterns of subsequent MRI progression in previously treated glioblastomas.

Methods—Twelve patients with a contrast-enhancing area suspicious for glioblastoma recurrence on MRI underwent PET scanning with the amino acid radiotracer alpha-[¹¹C]-methyl-L-tryptophan (AMT). Brain regions showing increased AMT uptake in and outside the contrast-enhancing volume were objectively delineated to include high uptake consistent with glioma (as defined by previous studies). Volume and tracer uptake of such non-enhancing PET+ regions were compared to spatial patterns and timing of subsequent progression of the contrast-enhancing lesion, as defined by serial surveillance MRI.

Results—Non-enhancing PET+ volumes varied widely across patients and extended up to 24 mm from the edge of MRI contrast enhancement. In 10 patients with clear progression of the contrast-enhancing lesion, the non-enhancing PET+ volumes predicted the location of new enhancement, which extended beyond the PET+ brain tissue in 6. In two patients, with no PET+ area beyond the initial contrast enhancement, MRI remained stable. There was a negative

Corresponding Author: Csaba Juhász, MD, PhD, PET Center and Translational Imaging Laboratory, Children's Hospital of Michigan, Depts. of Neurology and Pediatrics, Wayne State University School of Medicine, 3901 Beaubien Street, Detroit, MI 48201, Tel: 313-966-5136, Fax: 313-966-9228, juhasz@pet.wayne.edu.

Dr. Mittal and Dr. Juhász contributed to the manuscript equally.

Conflict of Interest: None of the authors report any conflict of interest or disclosure.

correlation between AMT uptake in non-enhancing brain and time to subsequent progression ($r = -0.77$, $p = 0.003$).

Conclusions—Amino acid PET imaging could complement MRI not only for detecting glioma recurrence but also predicting the location and timing of subsequent tumor progression. This could support decisions for surgical intervention or other targeted therapies for recurrent gliomas.

Keywords

Glioblastoma; tumor recurrence; MRI; positron emission tomography (PET); alpha- ^{11}C -methyl-L-tryptophan (AMT)

INTRODUCTION

Gliomas represent approximately 30% of all central nervous system tumors and 80% of all malignant brain tumors [1]. Glioblastomas have poor prognosis with a median survival of 15 months [1, 2]; however, a small percentage remains stable for a prolonged period of time after initial treatment. Treatment of high-grade gliomas includes surgery and chemoradiation therapy; however, malignant gliomas almost invariably recur in spite of aggressive management [3]. Conventional MRI, including T1-weighted gadolinium enhanced (T1-Gad), T2-weighted, or fluid-attenuated inversion recovery (FLAIR) sequences, is often not reliable in differentiation of recurrent tumor from treatment-induced tissue changes, such as radiation injury. Advanced MRI techniques including perfusion-weighted imaging (PWI), diffusion-weighted imaging (DWI), and MR spectroscopy (MRS) as well as positron emission tomography (PET) imaging have shown promise in the differentiation of glioma recurrence or progression from treatment-related changes [4]. Among PET techniques, imaging with radiolabeled amino acids can offer a powerful approach for non-invasive evaluation of brain tumors. Recent studies demonstrated that ^{11}C -methionine (MET), O-2- ^{18}F -fluoroethyl-L-tyrosine (FET), as well as 3,4-dihydroxy-6- ^{18}F -fluoro-L-phenylalanine (FDOPA) could be reliable techniques for detecting glioma recurrence and may complement MRI in clinical practice after further validation [5–12]. In a few comparative studies, amino acid PET performed better than ^{18}F -fluorodeoxy-glucose (FDG)-PET in post-treatment evaluation of malignant gliomas [7, 13–16].

Recently, our group evaluated the use of alpha- ^{11}C -methyl-L-tryptophan (AMT) as an amino acid PET tracer for evaluation of recurrent gliomas [7, 17, 18]. AMT is not incorporated into proteins but accumulates in gliomas partly due to metabolism via the immunosuppressive kynurenine pathway [7, 19, 20]. We demonstrated that AMT-PET can accurately differentiate between glioma recurrence and radiation injury in WHO grade II–IV gliomas [17]. We also reported that AMT uptake measured in areas with suspected high-grade glioma recurrence was a strong, independent predictor of survival [18]. In newly-diagnosed gliomas, we also observed increased AMT uptake extending beyond the MRI contrast-enhancing brain tumor mass, and histopathology from such non-enhancing regions demonstrated tumor cell infiltration [21, 22].

In the present study, we evaluated the clinical value of high AMT uptake in brain regions outside the contrast-enhancing tissue in post-treatment glioblastomas. We hypothesized that

such PET abnormalities could predict the location and timing of subsequent tumor progression as defined by serial contrast-enhanced MRI. Reliable detection of such areas at high risk for tumor progression may be useful for clinical decisions regarding targeted second-line treatments, such as reoperation, radiosurgery, or application of tumor treating alternating electric fields [23–25].

METHODS

Patient Population

We studied 12 patients with histologically-confirmed glioblastoma (age range: 46–80 years; mean: 61 years; Table 1), who had previously undergone maximal surgical resection followed by treatment with the Stupp regimen (radiotherapy plus concurrent daily temozolomide followed by adjuvant temozolomide) [26]. All patients underwent post-treatment AMT-PET imaging following an MRI that showed a contrast-enhancing area suspicious (but not definitive) for glioma progression as determined by a board-certified neuroradiologist. One of the following MRI patterns was observed: (i) slight increasing size of contrast enhancement on T1-Gad MRI with or without an increase in T2/FLAIR signal (n=8); (ii) small, new enhancing lesion without any other T1-Gad or T2/FLAIR signal abnormalities (n=2); (iii) enlarging area of increased T2/FLAIR signal with stable T1-Gad enhancement (n=1); or (iv) persistent enhancing lesion without recent progression (n=1). After AMT-PET, all 12 patients were followed for up to 2 years with serial MRI scans at 1- to 2-month intervals until clear progression of the contrast-enhancing lesions was noted. The study was approved by the Wayne State University Institutional Review Board with written informed consent obtained from all participants.

MRI Protocol

Diagnostic MRI with T1-Gad, T2, and FLAIR sequences, acquired shortly (mean: 14 days; range: 0–27 days) before AMT-PET, was used as the baseline studies. In addition, we also reviewed T1-Gad MRI scans acquired after AMT-PET, and further analyzed the first MRI that showed a clear progression (enlargement) of the contrast-enhancing lesion, in those patients where such a progression occurred within the 2-year follow-up period. MRI studies used for the analysis were performed on a Philips Achieva TX 3.0 Tesla magnet located at Karmanos Cancer Institute, Detroit, MI. The acquired brain tumor MRI protocol included: 4mm sagittal T1 turbo spin echo (TSE), 4mm axial pre- and post-contrast T1, T2, FLAIR, DWI, venous blood-oxygen-level dependent (BOLD) 3D gradient recalled echo (GRE) images; 1.0mm sagittal volume isotropic TSE acquisition (VISTA) FLAIR with coronal reformatted images; 1.0mm sagittal pre- and post-contrast T1 3D turbo field echo (TFE) with coronal and axial reformatted images; and PWI.

AMT-PET Scanning Protocol

PET studies were performed using a Siemens EXACT/HR whole-body positron emission tomograph (Siemens Medical Systems, Knoxville, TN). The AMT tracer was synthesized by using a high-yield procedure as outlined before [27]. The procedure for AMT-PET scanning has been described previously [21, 28]. In brief, after 6 h of fasting, AMT (37 MBq/kg) was injected intravenously. At 25 min after tracer injection, a dynamic emission scan of the brain

(7×5 min) was acquired. Measured attenuation correction, scatter, and decay correction was applied to all PET images. For visualization of AMT uptake, averaged activity images 30–55 min post-injection were created and converted to an AMT standardized uptake value (SUV) image. The PET image in plane resolution was 7.5 ± 0.4 mm at full-width half-maximum (FWHM) and 7.0 ± 0.5 mm FWHM in the axial direction.

Image Analysis

The 3D Slicer software version 3.6.3 (www.slicer.org) was used for threshold-based volume of interest (VOI) analysis [29]. First, AMT-PET and MR images acquired shortly before the PET were co-registered using the Fast Rigid Registration module [30]. Fused images were automatically resliced and resampled. The volume of increased AMT SUV in and around the contrast-enhancing area was determined based on a cutoff threshold (>65% increase as compared to contralateral cortical AMT SUV) that provided excellent accuracy to differentiate progressing high-grade gliomas associated with short survival vs. those with stable course and longer survival in our recent study [18]. We have also previously demonstrated that AMT cutoff thresholds above 36% would not detect voxels outside the MRI-detected (contrast-enhancing) tumor mass unless the tumor is infiltrated beyond the contrast-enhancing mass [21]. Voxels surviving this cutoff threshold were summed and their volume (i.e., PET+ volume) was expressed in cm^3 . In addition, the area of contrast enhancement was delineated on the T1-Gad images, and its volume (Gad+ volume) was also calculated [21]. Subsequently, we also calculated the volume of increased (above-threshold) AMT SUV located outside the contrast-enhancing volume (i.e., Gad–/PET+ volume). The mean (SUV_{mean}) and maximum (SUV_{max}) AMT SUV were also measured in this area. Furthermore, we measured the maximum distance (in mm) between the outer edge of the area with increased AMT uptake and the edge of the Gad+ volume. Subsequently, we repeated the volumetric analysis on the MRI scans showing radiographic evidence for clear T1-Gad progression (present in 10 patients), after these MR images were also co-registered with both the AMT-PET and the initial MR images (obtained prior to PET imaging). On the same MRI scans, showing T1-Gad tumor progression, we measured the Gad+ volume extending beyond the boundaries of the increased AMT uptake measured at baseline.

Statistical Analysis

The Wilcoxon signed rank test was utilized for the comparison of the PET+ volume extending beyond the Gad+ volume before vs. after MRI progression. Time to MRI progression was compared between subgroups showing different patterns of progression using Mann-Whitney U test. Further, AMT-PET and T1-Gad volume parameters as well as SUV_{mean} and SUV_{max} measured in the Gad–/PET+ areas were correlated with the time to progression using Spearman's rank correlations. The statistical analysis was performed using IBM SPSS Statistics for Windows, Version 19.0 (IBM Corp., Armonk, NY). A p value of less than 0.05 was considered significant.

RESULTS

AMT-PET Abnormalities

In all patients, at least one region with increased AMT uptake, as compared to normal contralateral cortex, was observed in and/or near the contrast-enhancing area (Table 2). In 11 patients, this increased AMT SUV exceeded the predefined cutoff threshold (1.65 lesion/cortex ratio), and its volume varied widely between 0.6 and 37.3 cm³ (median: 4.5 cm³) (Table 3). The PET+ area extended up to 24 mm (median: 10 mm) beyond the edge of the Gad+ region. The Gad-/PET+ volumes varied between 0 and 32.7 cm³ (median: 2.1 cm³) (Table 3). In one patient (#12), increased AMT SUV in the contrast-enhancing area did not reach the 1.65 cutoff threshold, therefore the measured PET+ volume was 0 in this patient. In another patient (#5), there were four different areas with contrast-enhancement in the left hemisphere (Table 2); in two of these regions, AMT SUV increases exceeded the cutoff threshold (and were included in Table 3), while the other two regions showed only milder increases.

Imaging Abnormalities after MRI Progression

Ten patients showed clear progression of the contrast-enhancing lesion(s), 1–17 months after the PET scan, while two patients (#11 and #12) showed no T1-Gad progression during the 2-year follow-up (Table 2). In those with T1-Gad MRI progression, new contrast-enhancement occurred preferentially in PET+ regions, with most of the Gad-/PET+ brain tissue becoming contrast enhancing (see detailed locations in Table 2); thus, the Gad-/PET+ volume decreased considerably to 0–1.4 cm³ after tumor progression (Table 3; median: 0.04 cm³; $p=0.005$ in Wilcoxon test). In 6 patients, the Gad+ region after progression not only invaded the PET+ brain tissue but extended considerably beyond it, with a widely varied volume (7.8–45 cm³) (Table 3; two examples shown on Figure 1); in the other 4 patients with tumor progression, the Gad+ volume expansion mirrored the PET+ volume but with no or minimal (<1 cm³) extension beyond the PET+ area (see example on Figure 2A). Time to MRI progression did not differ between these two subgroups ($p=0.9$).

In all 10 patients showing T1-Gad progression, subsequent MRI scans demonstrated further tumor progression, and two patients underwent reoperation. Histopathology verified the presence of active glioblastoma in the contrast-enhancing mass. All patients showed subsequent clinical progression and were deceased within 1–20 months.

In the two patients showing no T1-Gad progression during the 2-year follow-up, one patient (#11) showed a supra-threshold PET+ area, which was almost congruent with the bulk of the Gad+ lesion both at baseline and throughout the follow-up (Figure 2B); the other patient (#12) had only moderate AMT increase, not reaching the threshold, as described above.

Correlations between Imaging Abnormalities and Time to Progression

We found a negative correlation between both AMT SUV_{mean} and SUV_{max} and time to progression (after PET) (SUV_{mean}: $r=-0.77$, $p=0.003$; SUV_{max}: $r=-0.69$, $p=0.014$), indicating a faster progression in those with higher AMT uptake in the non-enhancing brain. Further inspection of the data showed that all patients with SUV_{max} > 4 ($n=8$) progressed

within about 5 months, while those with $SUV_{max} < 4$ were progression-free on serial MRI scans for at least 6 months. In contrast, volumes of Gad+ or Gad-/PET+ areas did not predict the time to subsequent radiographic progression ($p>0.2$).

DISCUSSION

Malignant gliomas almost invariably show high AMT uptake on PET before treatment [7, 21]. Our current study also demonstrated that increased AMT uptake in post-treatment glioblastomas commonly extends beyond the MRI contrast-enhancing area suspicious for tumor recurrence. Importantly, we found that subsequent progression of the contrast-enhancing area, consistent with glioma progression, encompassed the PET+ (originally contrast-negative) brain tissue, and, in some cases, extended beyond it. Thus, the location of increased amino acid uptake in contrast-negative areas could be a reliable predictor of the location of subsequent tumor progression. In addition, higher amino acid uptake in non-enhancing brain regions may predict faster tumor progression as detected by serial MRI scans.

Previous comparative studies between PET and histopathology findings in pre-treatment gliomas demonstrated that increased amino acid uptake on MET-PET and FET-PET can detect glioma-infiltrated brain tissue in non-enhancing regions [21, 31, 32]. In our previous study, we also demonstrated that increased AMT uptake outside MRI contrast-enhancing areas detect glioma-infiltrated tissue and differentiate it from non-tumoral MRI changes (such as peritumoral vasogenic edema) in patients with newly-diagnosed gliomas [21]. The PET findings were verified by histopathology performed in stereotactically-resected tissue samples. We also found that PET+ areas beyond the contrast-enhancing mass was significantly larger in glioblastomas compared with grade II-III gliomas [21]. In the present study of post-treatment gliomas, we used a strict threshold to delineate PET+ brain regions (65% increase as compared to contralateral normal cortex uptake) to exclude regions with radiation injury that could also cause a moderate increase of AMT uptake [17, 18]. Although we may have underestimated the area of tumor infiltration by using this strict threshold, we still found above-threshold AMT increases as far as 2.4 cm beyond the contrast-enhancing margin. The vast majority of glioma recurrences tend to develop within 2 cm from the initial enhancing tumor location [33, 34], but infiltrating glioma cells can be found 3 cm or further away from the contrast-enhancing margin [35]. In the present study, the subsequent extension of contrast-enhancement in non-enhancing areas with high AMT uptake strongly suggested that these PET+ regions indeed detected tumor-infiltrated brain before they became contrast-enhancing on MRI. It is also likely that glioma infiltration extended beyond the PET+ area to regions involved in subsequent MRI progression in some cases. Some of these areas could have been detected by using a lower AMT cutoff threshold. Further studies could determine an optimal threshold to detect glioma-infiltrated brain regions at highest risk for impending tumor progression. After further validation, reliable detection of glioma-infiltrated brain tissue beyond contrast-enhancing regions could be clinically useful to enhance neurosurgical planning for recurrent gliomas. Enhanced PET-assisted definition of the extent of brain-infiltrating tumor volume could also be useful for other targeted rescue therapies, such as the application of tumor treating electric fields [23, 24].

Another major finding of our study is the negative correlation between the AMT SUV and time to T1-Gad MRI progression, indicating that higher AMT uptake in non-enhancing areas could predict earlier glioma progression. Further inspection of the data also suggested that this may not be a linear correlation; rather, our limited data set suggests that an AMT SUV_{max} above 4 could be an imaging biomarker for imminent tumor progression (as early as within 1 month), which may prompt more frequent MRI follow-up or targeted interventions. In contrast, low AMT SUV_{max} (< 4 , in our study) beyond contrast enhancement is likely associated with a late progression or even a stable MRI during a 2-year follow-up. In clinical practice, the typical MRI follow-up interval is 2–3 months, which can be shortened in high-risk cases. In patients with subtle changes on serial MRI concerning for tumor progression, low amino acid uptake on PET may provide reassurance to continue the regular imaging follow-up and avoid unnecessary medical and/or surgical interventions.

Despite these encouraging results, our study has some inherent limitations. The study population was small; therefore, the findings will need further confirmation in a larger cohort of patients. In particular, larger, prospective studies could refine the role of amino acid PET imaging in subgroups showing various patterns of MRI progression. Future studies could also help optimize cutoff thresholds and test if other amino acid PET tracers provide similar or better results. AMT, similar to MET, has a short half-life (around 20 min) and is not as practical in a clinical setting as other amino acid PET radiotracers with longer half-lives such as FET or FDOPA. Also, while we compared AMT uptake to MRI contrast-enhancing regions, it would be interesting to correlate the PET findings with advanced MRI techniques such as PWI. Current response assessment criteria rely heavily on contrast-enhanced MRI [36], which is widely used clinically for monitoring post-treatment glioma progression. Although advanced MRI modalities such as PWI and MRS are increasingly utilized in clinical practice, the number of comparative studies with amino acid PET remains limited. In a recent study, comparing FET-PET and PWI in patients with post-treatment gliomas, the two modalities provided substantially different tumor delineation [37]. This indicates that amino acid PET can detect metabolically active tumor showing no perfusion abnormality; therefore, these two imaging modalities could provide complementary information to assess the risk of imminent glioma progression during the post-treatment monitoring period.

In summary, we demonstrated that amino acid PET imaging with AMT could complement conventional T1-Gad MRI not only for detecting glioma recurrence but also predicting the location and timing of subsequent tumor progression. Thus, evaluation of amino acid uptake in patients with suspected glioma recurrence may be useful to guide surgical interventions or other targeted therapies to optimize treatment effects in patients with recurrent malignant gliomas.

Acknowledgments

Funding: The study was supported by a grant (CA123451 to C.J. and S.M.) from the National Cancer Institute; a grant from the Fund for Medical Research and Education, Wayne State University School of Medicine (to S.M.); and Strategic Research Initiative Grant from the Karmanos Cancer Institute (to S.M. and C.J.).

The study was supported by a grant (R01 CA123451 to C.J. and S.M.) from the National Cancer Institute; a grant from the Fund for Medical Research and Education, Wayne State University School of Medicine (to S.M.); and a Strategic Research Initiative Grant from the Karmanos Cancer Institute (to S.M. and C.J.). We thank Janet Barger, RN, Kelly Forcucci, RN and Cathie Germain, MA for assisting patient recruitment and scheduling. We also thank William J. Kupsky, MD, who performed the clinical histopathology evaluation of the tumor specimens. We are grateful to the entire staff at the PET Center, Children's Hospital of Michigan, who provided invaluable technical help in performing the PET scans.

References

1. Omuro A, DeAngelis LM. Glioblastoma and other malignant gliomas: a clinical review. *JAMA*. 2013; 310:1842–1850. [PubMed: 24193082]
2. Stupp R, Hegi ME, Mason WP, van den Bent MJ, Taphoorn MJ, Janzer RC, Ludwin SK, Allgeier A, Fisher B, Belanger K, Hau P, Brandes AA, Gijtenbeek J, Marosi C, Vecht CJ, Mokhtari K, Wesseling P, Villa S, Eisenhauer E, Gorlia T, Weller M, Lacombe D, Cairncross JG, Mirimanoff RO, European Organisation for R, Treatment of Cancer Brain T, Radiation Oncology G, National Cancer Institute of Canada Clinical Trials G. Effects of radiotherapy with concomitant and adjuvant temozolomide versus radiotherapy alone on survival in glioblastoma in a randomised phase III study: 5-year analysis of the EORTC-NCIC trial. *Lancet Oncol*. 2009; 10:459–466. [PubMed: 19269895]
3. Xie Q, Mittal S, Berens ME. Targeting adaptive glioblastoma: an overview of proliferation and invasion. *Neuro Oncol*. 2014; 16:1575–1584. [PubMed: 25082799]
4. Dhermain FG, Hau P, Lanfermann H, Jacobs AH, van den Bent MJ. Advanced MRI and PET imaging for assessment of treatment response in patients with gliomas. *Lancet Neurol*. 2010; 9:906–920. [PubMed: 20705518]
5. Nihashi T, Dahabreh IJ, Terasawa T. PET in the clinical management of glioma: evidence map. *AJR Am J Roentgenol*. 2013; 200:W654–660. [PubMed: 23701099]
6. Gulyas B, Halldin C. New PET radiopharmaceuticals beyond FDG for brain tumor imaging. *Q J Nucl Med Mol Imaging*. 2012; 56:173–190. [PubMed: 22617239]
7. Juhasz C, Dwivedi S, Kamson DO, Michelhaugh SK, Mittal S. Comparison of amino acid positron emission tomographic radiotracers for molecular imaging of primary and metastatic brain tumors. *Mol Imaging*. 2014; 13doi: 10.2310/7290.2014.00015
8. Terakawa Y, Tsuyuguchi N, Iwai Y, Yamanaka K, Higashiyama S, Takami T, Ohata K. Diagnostic accuracy of ^{11}C -methionine PET for differentiation of recurrent brain tumors from radiation necrosis after radiotherapy. *J Nucl Med*. 2008; 49:694–699. [PubMed: 18413375]
9. Nariai T, Tanaka Y, Wakimoto H, Aoyagi M, Tamaki M, Ishiwata K, Senda M, Ishii K, Hirakawa K, Ohno K. Usefulness of L-[methyl- ^{11}C] methionine-positron emission tomography as a biological monitoring tool in the treatment of glioma. *J Neurosurg*. 2005; 103:498–507. [PubMed: 16235683]
10. Rachinger W, Goetz C, Popperl G, Gildehaus FJ, Kreth FW, Holtmannspotter M, Herms J, Koch W, Tatsch K, Tonn JC. Positron emission tomography with O-(2-[^{18}F]fluoroethyl)-L-tyrosine versus magnetic resonance imaging in the diagnosis of recurrent gliomas. *Neurosurgery*. 2005; 57:505–511. [PubMed: 16145529]
11. Weber WA, Wester HJ, Grosu AL, Herz M, Dzewas B, Feldmann HJ, Molls M, Stocklin G, Schwaiger M. O-(2-[^{18}F]fluoroethyl)-L-tyrosine and L-[methyl- ^{11}C]methionine uptake in brain tumours: initial results of a comparative study. *Eur J Nucl Med*. 2000; 27:542–549. [PubMed: 10853810]
12. Grosu AL, Astner ST, Riedel E, Nieder C, Wiedenmann N, Heinemann F, Schwaiger M, Molls M, Wester HJ, Weber WA. An interindividual comparison of O-(2-[^{18}F]fluoroethyl)-L-tyrosine (FET)- and L-[methyl- ^{11}C]methionine (MET)-PET in patients with brain gliomas and metastases. *Int J Radiat Oncol Biol Phys*. 2011; 81:1049–1058. [PubMed: 21570201]
13. Chung JK, Kim YK, Kim SK, Lee YJ, Paek S, Yeo JS, Jeong JM, Lee DS, Jung HW, Lee MC. Usefulness of ^{11}C -methionine PET in the evaluation of brain lesions that are hypo- or isometabolic on ^{18}F -FDG PET. *Eur J Nucl Med Mol Imaging*. 2002; 29:176–182. [PubMed: 11926379]
14. Kim S, Chung JK, Im SH, Jeong JM, Lee DS, Kim DG, Jung HW, Lee MC. ^{11}C -methionine PET as a prognostic marker in patients with glioma: comparison with ^{18}F -FDG PET. *Eur J Nucl Med Mol Imaging*. 2005; 32:52–59. [PubMed: 15309332]

15. Lau EW, Drummond KJ, Ware RE, Drummond E, Hogg A, Ryan G, Grigg A, Callahan J, Hicks RJ. Comparative PET study using F-¹⁸ FET and F-¹⁸ FDG for the evaluation of patients with suspected brain tumour. *J Clin Neurosci*. 2010; 17:43–49. [PubMed: 20004582]
16. Plotkin M, Blechschmidt C, Auf G, Nyuyki F, Geworski L, Denecke T, Brenner W, Stockhammer F. Comparison of F-¹⁸ FET-PET with F-¹⁸ FDG-PET for biopsy planning of non-contrast-enhancing gliomas. *Eur Radiol*. 2010; 20:2496–2502. [PubMed: 20521054]
17. Alkonyi B, Barger GR, Mittal S, Muzik O, Chugani DC, Bahl G, Robinette NL, Kupsky WJ, Chakraborty PK, Juhasz C. Accurate differentiation of recurrent gliomas from radiation injury by kinetic analysis of alpha-¹¹C-methyl-L-tryptophan PET. *J Nucl Med*. 2012; 53:1058–1064. [PubMed: 22653792]
18. Kamson DO, Mittal S, Robinette NL, Muzik O, Kupsky WJ, Barger GR, Juhasz C. Increased tryptophan uptake on PET has strong independent prognostic value in patients with a previously treated high-grade glioma. *Neuro Oncol*. 2014; 16:1373–1383. [PubMed: 24670609]
19. Chugani DC, Muzik O. Alpha[¹¹C]methyl-L-tryptophan PET maps brain serotonin synthesis and kynurenine pathway metabolism. *J Cereb Blood Flow Metab*. 2000; 20:2–9. [PubMed: 10616786]
20. Batista CE, Juhasz C, Muzik O, Kupsky WJ, Barger G, Chugani HT, Mittal S, Sood S, Chakraborty PK, Chugani DC. Imaging correlates of differential expression of indoleamine 2,3-dioxygenase in human brain tumors. *Mol Imaging Biol*. 2009; 11:460–466. [PubMed: 19434461]
21. Kamson DO, Juhasz C, Buth A, Kupsky WJ, Barger GR, Chakraborty PK, Muzik O, Mittal S. Tryptophan PET in pretreatment delineation of newly-diagnosed gliomas: MRI and histopathologic correlates. *J Neurooncol*. 2013; 112:121–132. [PubMed: 23299463]
22. Jeong JW, Juhasz C, Mittal S, Bosnyak E, Kamson DO, Barger GR, Robinette NL, Kupsky WJ, Chugani DC. Multi-modal imaging of tumor cellularity and Tryptophan metabolism in human Gliomas. *Cancer Imaging*. 2015; 15:10. doi: 10.1186/s40644-015-0045-1 [PubMed: 26245742]
23. Kirson ED, Dbaly V, Tovarys F, Vymazal J, Soustiel JF, Itzhaki A, Mordechovich D, Steinberg-Shapira S, Gurvich Z, Schneiderman R, Wasserman Y, Salzberg M, Ryffel B, Goldsher D, Dekel E, Palti Y. Alternating electric fields arrest cell proliferation in animal tumor models and human brain tumors. *Proc Natl Acad Sci U S A*. 2007; 104:10152–10157. [PubMed: 17551011]
24. Stupp R, Wong ET, Kanner AA, Steinberg D, Engelhard H, Heidecke V, Kirson ED, Taillibert S, Liebermann F, Dbaly V, Ram Z, Villano JL, Rainov N, Weinberg U, Schiff D, Kunschner L, Raizer J, Honnorat J, Sloan A, Malkin M, Landolfi JC, Payer F, Mehdorn M, Weil RJ, Pannullo SC, Westphal M, Smrcka M, Chin L, Kostron H, Hofer S, Bruce J, Cosgrove R, Paleologous N, Palti Y, Gutin PH. NovoTTF-100A versus physician's choice chemotherapy in recurrent glioblastoma: a randomised phase III trial of a novel treatment modality. *Eur J Cancer*. 2012; 48:2192–2202. [PubMed: 22608262]
25. Kim HR, Kim KH, Kong DS, Seol HJ, Nam DH, Lim do H, Lee JI. Outcome of salvage treatment for recurrent glioblastoma. *J Clin Neurosci*. 2015; 22:468–473. [PubMed: 25595963]
26. Stupp R, Mason WP, van den Bent MJ, Weller M, Fisher B, Taphoorn MJ, Belanger K, Brandes AA, Marosi C, Bogdahn U, Curschmann J, Janzer RC, Ludwin SK, Gorlia T, Allgeier A, Lacombe D, Cairncross JG, Eisenhauer E, Mirimanoff RO. European Organisation for R, Treatment of Cancer Brain T, Radiotherapy G, National Cancer Institute of Canada Clinical Trials G. Radiotherapy plus concomitant and adjuvant temozolomide for glioblastoma. *N Engl J Med*. 2005; 352:987–996. [PubMed: 15758009]
27. Chakraborty PK, Mangner TJ, Chugani DC, Muzik O, Chugani HT. A high-yield and simplified procedure for the synthesis of alpha-[¹¹C]methyl-L-tryptophan. *Nucl Med Biol*. 1996; 23:1005–1008. [PubMed: 9004289]
28. Juhasz C, Chugani DC, Muzik O, Wu D, Sloan AE, Barger G, Watson C, Shah AK, Sood S, Ergun EL, Mangner TJ, Chakraborty PK, Kupsky WJ, Chugani HT. In vivo uptake and metabolism of alpha[¹¹C]methyl-L-tryptophan in human brain tumors. *J Cereb Blood Flow Metab*. 2006; 26:345–357. [PubMed: 16079785]
29. Kikinis R, Pieper S. 3D Slicer as a tool for interactive brain tumor segmentation. *Conf Proc IEEE Eng Med Biol Soc*. 2011; 2011:6982–6984. [PubMed: 22255945]
30. Mattes D, Haynor DR, Vesselle H, Lewellen TK, Eubank W. PET-CT image registration in the chest using free-form deformations. *IEEE Trans Med Imaging*. 2003; 22:120–128. [PubMed: 12703765]

31. Kracht LW, Miletic H, Busch S, Jacobs AH, Voges J, Hoevels M, Klein JC, Herholz K, Heiss WD. Delineation of brain tumor extent with [¹¹C]L-methionine positron emission tomography: local comparison with stereotactic histopathology. *Clin Cancer Res.* 2004; 10:7163–7170. [PubMed: 15534088]
32. Pauleit D, Stoffels G, Schaden W, Hamacher K, Bauer D, Tellmann L, Herzog H, Broer S, Coenen HH, Langen KJ. PET with O-(2-¹⁸F-Fluoroethyl)-L-Tyrosine in peripheral tumors: first clinical results. *J Nucl Med.* 2005; 46:411–416. [PubMed: 15750152]
33. Wallner KE, Galicich JH, Krol G, Arbit E, Malkin MG. Patterns of failure following treatment for glioblastoma multiforme and anaplastic astrocytoma. *Int J Radiat Oncol Biol Phys.* 1989; 16:1405–1409. [PubMed: 2542195]
34. Oppitz U, Maessen D, Zunterer H, Richter S, Flentje M. 3D-recurrence-patterns of glioblastomas after CT-planned postoperative irradiation. *Radiother Oncol.* 1999; 53:53–57. [PubMed: 10624854]
35. Burger PC, Heinz ER, Shibata T, Kleihues P. Topographic anatomy and CT correlations in the untreated glioblastoma multiforme. *J Neurosurg.* 1988; 68:698–704. [PubMed: 2833587]
36. Wen PY, Macdonald DR, Reardon DA, Cloughesy TF, Sorensen AG, Galanis E, Degroot J, Wick W, Gilbert MR, Lassman AB, Tsien C, Mikkelsen T, Wong ET, Chamberlain MC, Stupp R, Lamborn KR, Vogelbaum MA, van den Bent MJ, Chang SM. Updated response assessment criteria for high-grade gliomas: response assessment in neuro-oncology working group. *J Clin Oncol.* 2010; 28:1963–1972. [PubMed: 20231676]
37. Filss CP, Galldiks N, Stoffels G, Sabel M, Wittsack HJ, Turowski B, Antoch G, Zhang K, Fink GR, Coenen HH, Shah NJ, Herzog H, Langen KJ. Comparison of ¹⁸F-FET PET and perfusion-weighted MR imaging: a PET/MR imaging hybrid study in patients with brain tumors. *J Nucl Med.* 2014; 55:540–545. [PubMed: 24578243]

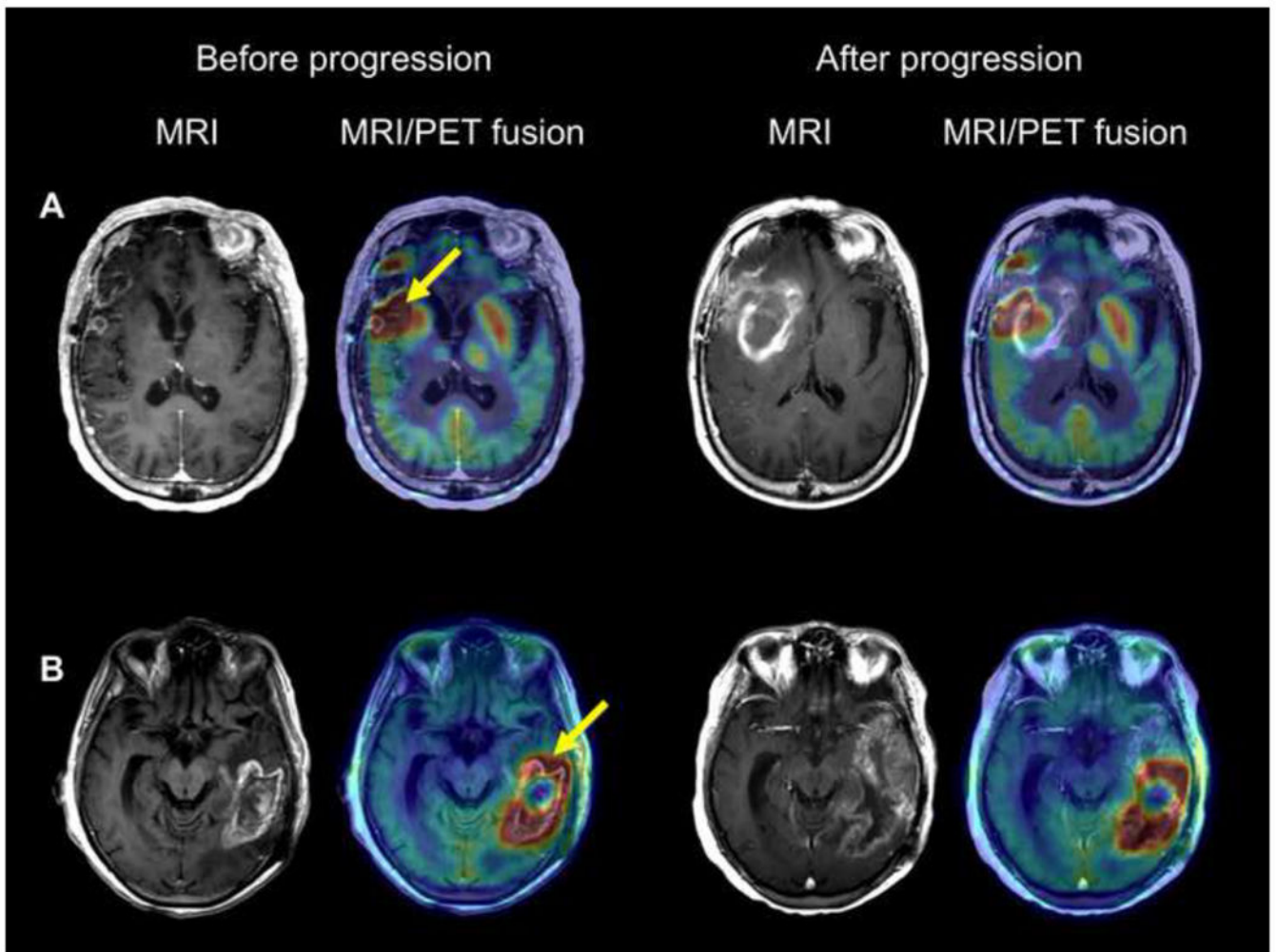


Figure 1. T1-Gad MRI and co-registered MRI/AMT-PET fusion images of two patients with tumor progression beyond the PET+ region

(A) Patient #1 showed contrast-enhancement and high AMT uptake at baseline in the right inferior frontal and anterior temporal lobes. The temporal lobe area with AMT increase extended well beyond the contrast-enhancing region medially toward the basal ganglia (arrow), with a maximum standardized uptake value (SUV_{max}) of 5.7. Follow-up MRI in one month showed a rapid progression with a large medial extension of the contrast-enhancing lesion encompassing and extending beyond the baseline PET+ area.

(B) Patient #8 had a large contrast-enhancing area and high AMT uptake in the left temporal region. The PET+ area extended anterior to the Gad+ lesion (arrow), with an SUV_{max} of 5.4. T1-Gad MRI 5 months later showed extension of the contrast enhancement into the anterior temporal lobe encompassing and extending beyond the baseline PET+ region.

Figure2A

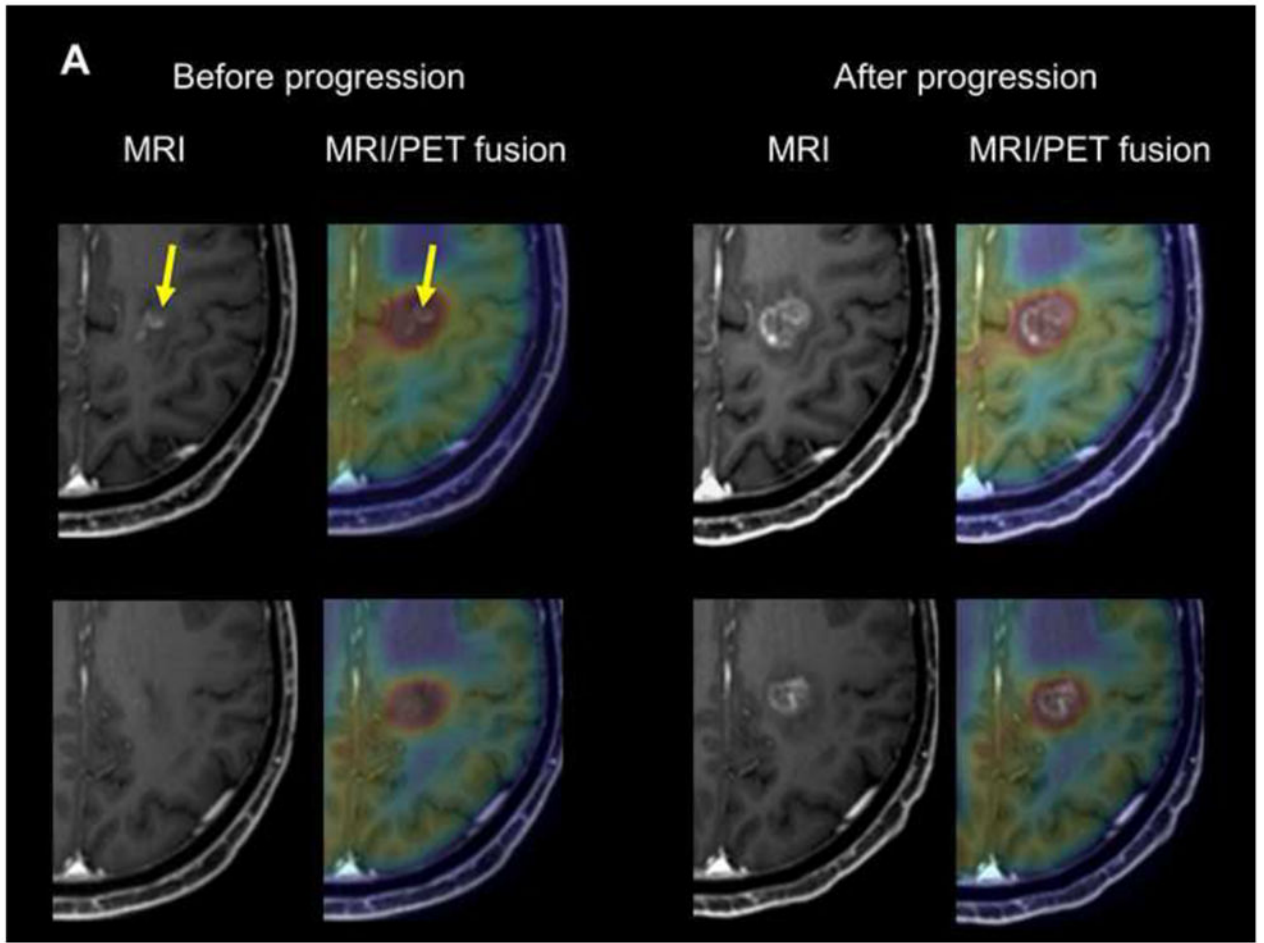


Figure 2B

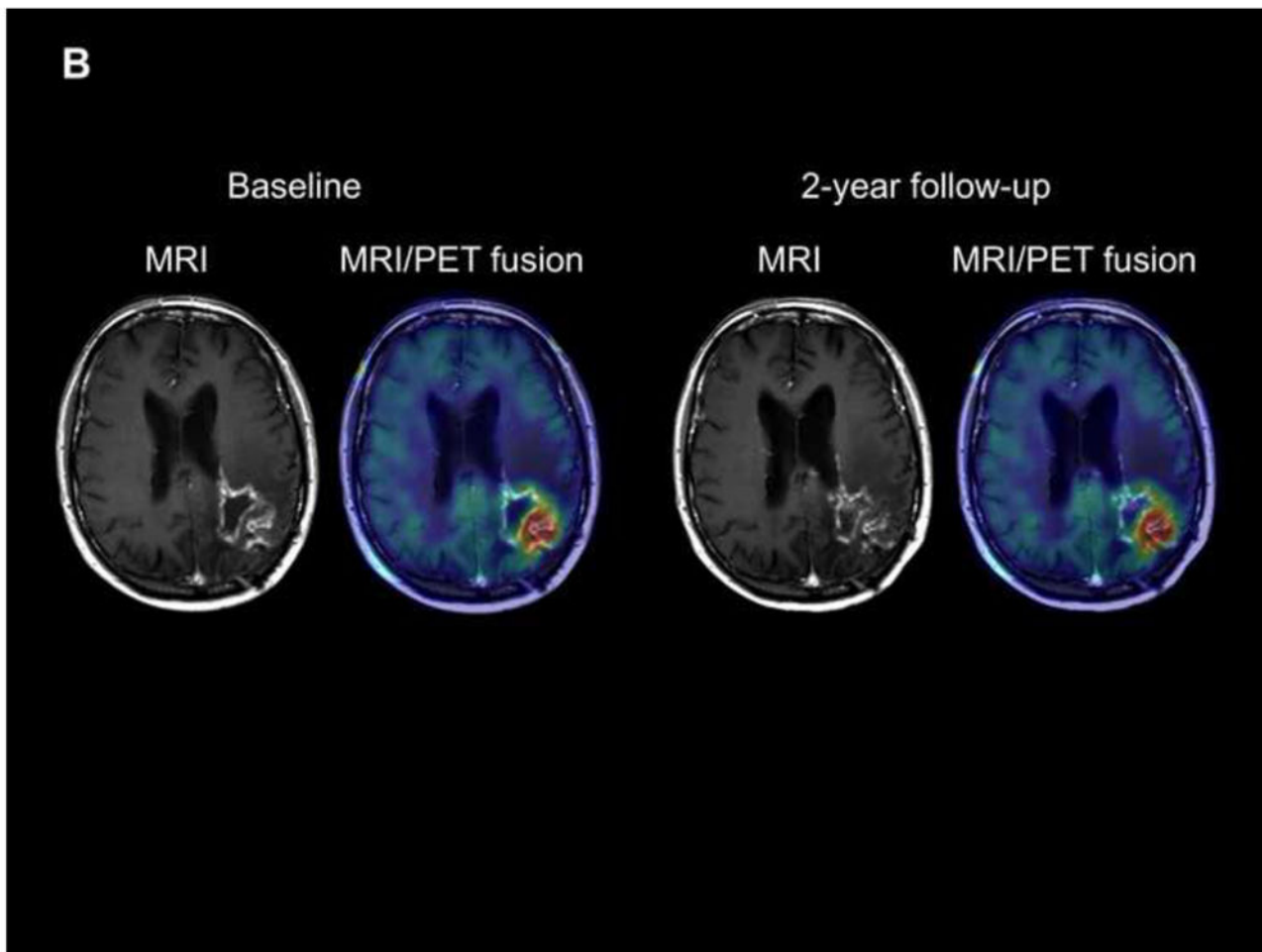


Figure 2. T1-Gad MRI and co-registered MRI/AMT-PET fusion images of two patients with progression of the enhancing area within the PET+ region

(A) T1-Gad MRI and co-registered MRI/AMT-PET fusion images of patient #2 showing a left medial fronto-parietal contrast-enhancing lesion (arrows) suspicious for glioblastoma recurrence 4 months after initial treatment. High AMT uptake was seen in the same region (upper panel), extending superior (and also inferior and lateral) to the contrast-enhancing lesion (lower panel), with an SUV_{max} of 4.7. After MRI progression, 1 month later, the Gad + mass grew into and filled the original PET+/Gad- area.

(B) T1-Gad MRI and co-registered MRI/AMT-PET fusion images of patient #11 showing a left parieto-occipital contrast-enhancing lesion. The PET+ area was almost congruent with the bulk of the Gad+ lesion, which showed no progression during the 2-year follow-up. SUV_{max} was below 4 (3.8).

Table 1

Clinical data of the 12 patients with previously treated glioblastoma

Patient No.	Gender	Age (years)	Time between initial treatment to AMT-PET (months)	Time to MRI progression after AMT-PET (days)
1	F	68	4	30
2	M	46	4	31
3	F	59	6	68
4	F	63	17	74
5	M	49	5	105
6	M	59	16	112
7	F	46	20	137
8	F	79	8	160
9	M	58	11	184
10	F	59	27	510
11	M	80	11	no progression
12	M	67	16	no progression

Table 2

Locations of MRI contrast enhancing lesions at baseline and corresponding areas of increased AMT uptake (as compared to normal cortex, on visual inspection); extension of PET+ regions beyond contrast enhancement, if present, is indicated in parentheses. In the last column, directions of the expansion of the contrast enhancing lesion are shown: directions where contrast-enhancement extended into previous PET+/Gad- regions are indicated with bolded letters

Patient No.	Imaging before MRI progression		MRI progression
	Contrast enhancement	Increased AMT uptake	
1	R ant/sup T	R ant/sup T (ext. inf)	inf, med
2	L F-P	L F-P (ext. sup, inf, lat)	sup, inf, lat
3	R inf F	R inf F (ext. ant)	ant, post, med
4	R med T	R med T (ext. post)	post
5*	L inf/med T	L inf/med T (ext. ant, lat)	ant, lat
	L splenium	L splenium (mild)	med
	none	L lat T (cortical, mild)	lat (subcortical)
	L+R F base	F base (overlap)	no progression
6	R lat T	R lat T (ext. sup)	sup, med, ant
7	R sup F-P	R sup F-P (ext. sup, post, med)	sup, post, med
8	L T	L T (ext. ant)	ant
9	R F-P	R F-P (ext. sup, post)	sup, post
10	L P-O	L P-O	post, lat, inf, ant
11	L P	L P	no progression
12	R ant T	R ant T (mild)	no progression

R=right, L=left, inf=inferior, sup=superior, med=medial, lat=lateral, ant=anterior, post=posterior,

F=frontal, P=parietal, T=temporal, O=occipital; ext.=extending (beyond contrast enhancement)

* This patient had three separate contrast-enhancing lesions at baseline: two of these showed eventual progression, while a fourth contrast-enhancing lesion emerged at follow-up in the vicinity of a lateral temporal area showing a mild increase of AMT uptake at baseline.

Table 3

Quantitative imaging results

Patient No.	PET+ total volume (cm ³)	PET+ volume beyond Gad+ area		AMT SUV _{mean} /SUV _{max} in Gad+ area	PET+ max. distance beyond Gad+ area (mm)	Gad+ volume beyond PET+ after progression (cm ³)
		Before Gad progression (cm ³)	After Gad progression (cm ³)			
1	4.2	3.5	0.3	4.7/5.7	21	9.1
2	0.6	0.5	0	4.2/4.7	5	0
3	3.8	0.8	0	7.0/8.5	6	14.3
4	5.8	2.3	0	4.2/4.8	11	45
5	33.7	5.9	0.6	3.2/6.8	15	0.6
	2.5	0	no progression	2.9/3.6	0	no progression
6	6.5	2.9	1.3	3.8/4.6	13	7.8
7	9.7	7.9	1.4	4.6/6.9	11	0
8	37.3	32.7	0	3.8/5.4	24	12.2
9	2.7	1.8	0	3.1/3.7	10	0.8
10	0.9	0.5	0.1	3.5/3.6	7	13.1
11	4.5	0	no progression	3.5/3.8	0	no progression
12	0	0	no progression	2.4/2.5	0	no progression

AMT: alpha-[¹¹C]-methyl-L-tryptophan, SUV: standardized uptake value; Gad: gadolinium